Appl Microbiol Biotechnol
DOI 10.1007/s00253-015-6630-1

The production of ω-hydroxy palmitic acid using fatty acid metabolism and cofactor optimization in *Escherichia coli*

Changmin Sung[1,3] · Eunok Jung[2,3] · Kwon-Young Choi[4] · Jin-hyung Bae[2] · Minsuk Kim[2] · Joonwon Kim[2] · Eun-Jung Kim[3] · Pyoung Il Kim[5] · Byung-Gee Kim[1,2,3,6]

Received: 26 December 2014 / Revised: 9 April 2015 / Accepted: 15 April 2015

Abstract Hydroxylated fatty acids (HFAs) are used as important precursors for bulk and fine chemicals in the chemical industry. Here, to overproduce long-chain (C16–C18) fatty acids and hydroxy fatty acid, their biosynthetic pathways including thioesterase (*Lreu_0335*) from *Lactobacillus reuteri* DSM20016, β-hydroxyacyl-ACP dehydratase (*fabZ*) from *Escherichia coli*, and a P450 system (i.e., CYP153A from *Marinobacter aquaeolei* VT8 and *cam*A/*cam*B from *Pseudomonas putida* ATCC17453) were overexpressed. Acyl-CoA synthase (*fad*D) involved in fatty acid degradation by β-oxidation was also deleted in *E. coli* BW25113. The engineered *E. coli* FFA4 strain without the P450 system could produce 503.0 mg/l of palmitic (C_{16}) and 508.4 mg/l of stearic (C_{18}) acids, of which the amounts are ca. 1.6- and 2.3-fold higher than those of the wild type. On the other hand, the *E. coli* HFA4 strain including the P450 system for ω-hydroxylation could produce 211.7 mg/l of ω-hydroxy palmitic acid, which was 42.1±0.1 % of the generated palmitic acid, indicating that the hydroxylation reaction was the rate-determining step for the HFA production. For the maximum production of ω-hydroxy palmitic acid, NADH, i.e., an essential cofactor for P450 reaction, was overproduced by the integration of NAD^+-dependent formate dehydrogenase (FDH) from *Candida boidinii* into *E. coli* chromosome and the deletion of alcohol dehydrogenase (ADH). Finally, the NADH-level-optimized *E. coli* strain produced 610 mg/l of ω-hydroxy palmitic acid (ω-HPA), which was almost a three-fold increase in its yield compared to the same strain without NADH overproduction.

Keywords Free fatty acid · Hydroxy fatty acid · Metabolic engineering · P450 monooxygenase · Cofactor optimization

Electronic supplementary material The online version of this article (doi:10.1007/s00253-015-6630-1) contains supplementary material, which is available to authorized users.

✉ Byung-Gee Kim
byungkim@snu.ac.kr

[1] Interdisciplinary Program for Bioengineering, Seoul National University, Seoul, South Korea

[2] School of Chemical and Biological Engineering, Institute of Bioengineering, Seoul National University, Seoul, South Korea

[3] School of Chemical and Biological Engineering, Institute of Molecular Biology and Genetics, Seoul National University, Seoul, South Korea

[4] Department of Environmental Engineering, College of Engineering, Ajou University, Suwon, Gyeonggi-do, South Korea

[5] Bio Control Research Institute, JBF, 495 Ipmyeon-ro, Ipmyeon, Gokseong-gun, Jeonnam, South Korea

[6] Present address: Seoul National University, #302-613, Gwanak_599, Gwanak-ro, Gwanak-gu, Seoul, South Korea

Introduction

The recent energy shortage and the increase of CO_2 elevating the global warming effect have motivated the use of renewable resources, especially from biomass, to produce energy and commodity bulk chemicals (Handke et al. 2011; Nawabi et al. 2011; Peralta-Yahya et al. 2012). Free fatty acids (FFAs) are present as a component of cell lipids and have been used as a good starting material for bioplastics, functional chemicals, and food ingredients (Kim and Oh 2013). FFAs are produced by hydrolysis of oils from palm tree (Voll et al. 2012) and microalgae (Yan et al. 2011). Biodiesel from oils can be simply made as fatty acid ester forms, generating one-third molar equivalent amounts of glycerol as by-products (Shirazi et al. 2013). Various functional chemicals can also be produced by

Published online: 09 May 2015

further chemical modifications of FFAs. Another interesting route for FFAs is the direct synthesis of FFAs from glucose, sugar cane, and lignocelluloses (Naik et al. 2010), where significant scientific challenges remain for the further improvement of yield and productivity using new approaches of systems biology (Wang et al. 2013) and metabolic engineering with synthetic biology tools (Luo et al. 2013).

To synthesize FFAs directly from glucose, many research groups have attempted to develop and engineer yeast (Jin et al. 2013) and *Escherichia coli* strains as production host cells (Liu et al. 2010; Lu et al. 2008). According to these works, releasing fatty acyl groups from acyl carrier protein (ACP) through amplification of thioesterase (TE), or the disruption of the FFA β-oxidation pathway by the deletion of acyl-CoA synthase (*fad*D), functioning as the first-step enzyme of the β-oxidation pathway, is critical for efficient synthesis of FFAs (Lu et al. 2008; Jeon 2012). In addition, the engineering strategy of transaldolase A (*tal*A) disruption resulted in higher FFA yield up to 20 % by disconnecting the link between the pentose phosphate pathway and the hexose diphosphate pathway, thereby increasing the intracellular NADPH pool (Ranganathan et al. 2012).

Since the construction of biorefinery from renewable resources is becoming a very attractive research subject, various hydroxylated fatty acid (HFA) productions using cellulosic materials yielding glucose have become more interesting challenges in white biotechnology. Various HFAs can easily be produced by either catalyst-dependent chemical synthesis or biotransformation from FFA (Kim and Oh 2013). In biotransformation, several strategies have been developed to introduce the hydroxyl group at specific positions in long carbon chains of FFA: (i) direct introduction of a hydroxyl group at specific sites using hydroxylase and P450 (Silke Schneider et al. 1998; Matsunaga et al. 1996); (ii) reduction to generate a double bond at specific sites and subsequent hydration in the double bond using desaturase and hydratase (Joo et al. 2012), respectively; (iii) reduction to generate a double bond at specific sites and subsequent epoxidation, followed by hydrolysis using desaturase, epoxidase, and epoxide hydrolase (Jung et al. 2012); and (iv) lipoxygenase and diol synthase in the presence of (*cis*,*cis*)-double bonds and a double bond generating dihydroxy form (Brash 1999; Jerneren and Oliw 2012), respectively. Among them, one of the most challenging steps studied till now is the control of the terminal position hydroxylation of long-chain FFA, called ω-hydroxylation (Van Bogaert et al. 2011), since for other chemical catalysts and/or enzymes except P450s and non-heme di-iron monooxygenase (Schrewe et al. 2014), it is difficult to carry out such reaction.

Recently, P450s from marine bacteria such as *Marinobacter aquaeolei* VT8 were successfully screened and used for long-chain HFA bioconversion from their corresponding FFAs (Kubota et al. 2005). The same enzyme system can be applied for the synthesis of ω-HFA from glucose, so that a cytochrome P450 monooxygenase enzyme (CYP153A) reaction with high specificity for ω-hydroxylation at long-chain FFAs such as palmitic (C_{16}) acid was combined with the FFA biosynthesis pathway present in the *E. coli* host system. To improve such P450 monooxygenase reaction system, a rate-limiting step for the biosynthesis of ω-HFA not only for high P450 activity but also for the supply of sufficient reducing power cofactors is essential for the maximum production of ω-HFA. To supply sufficient reducing power, in general, genetic engineering for blocking cofactor-consuming pathways and the introduction of biosynthetic pathways have been attempted in industrial host development (Choi et al. 2014). Besides the maximization of appropriate reducing power for the P450 reaction system, the host cell itself has an endogenously preferred NAD(P)H/NAD(P)$^+$ ratio to balance cell growth and biosynthesis of target products. Therefore, to produce target products in heterologous recombinant *E. coli*, the changes in NAD(P)H/NAD(P)$^+$ ratio can dramatically affect the productivity and yield of target products.

In this study, an *E. coli* strain was developed to produce ω-HFA from glucose without exogenous feeding of FFA. First, the FFA degradation pathways, i.e., the fatty acyl-CoA synthase (*fad*D) and transaldolase A (*tal*A), were disrupted in order to increase the intracellular pool of FFAs. Also, thioesterase (*Lreu_0335*) from *Lactobacillus reuteri* DSM 20016 and β-hydroxymyristoyl acyl carrier protein (ACP) dehydratase (*fab*Z) from *E. coli* were overexpressed to drive carbon flux into a synthesis of a long-chain (C_{16} and C_{18}) FFA. To subsequently convert the FFAs into the corresponding HFAs, FFA ω-hydroxylase (CYP153A) from *Marinobacter aqueolei* and electron-transferring protein (CamAB) from *Pseudomonas putida* were overexpressed. To supply enough NADH for electron transfer to CYP153A, NAD$^+$-dependent formate dehydrogenase from *Candida boidinii* was integrated into *E. coli* chromosome, while alcohol dehydrogenase (ADH) of *E. coli* was deleted for blocking a NADH consumption pathway. Compared to the result previously reported, much higher yield and productivity of ω-HFA synthesis were achieved using the designed strain, and the product (HFAs) could be used as valuable chemical feed stocks (Bhattarai et al. 2013; Wang et al. 2012).

Materials and methods

Bacterial strains and materials

All strains, vectors, and plasmids used in this study are listed in Table 1. *E. coli* DH5α (Invitrogen, USA) was used for plasmid cloning and propagation, while *E. coli* BW25113 (DE3) was used for free fatty acid and hydroxyl fatty acid production. Vectors, pETDuet-1, and pCDFDuet-1 (Novagen,

Table 1 Genetic manipulation and construction of plasmid lists for FFA and HPA production

Strains/plasmids	Description
Stains	
Escherichia coli DH5α	General cloning host
BW25113(DE3)	F-, DE(*ara*D-*ara*B)567, acZ4787(del)::*rrn*B-3, LAM-, rph-1, DE(*rha*D-*rha*B)568, hsdR514
FFA1	BW25113(DE3) Δ*fad*D
FFA2	BW25113(DE3) Δ*fad*D Δ*tal*A
FFA3	BW25113(DE3) Δ*fad*D+pTEZ
FFA4	BW25113(DE3) Δ*fad*D Δ*tal*A+pTEZ
HFA1	BW25113(DE3) Δ*fad*D+pCYPAB
HFA2	BW25113(DE3) Δ*fad*D Δ*tal*A+pCYPAB
HFA3	BW25113(DE3) Δ*fad*D+pTEZ+pCYPAB
HFA4	BW25113(DE3) Δ*fad*D Δ*tal*A+pTEZ+pCYPAB
HFA5	BW25113(DE3) Δ*fad*D+pCYPR
HFNA	BW25113(DE3) Δ*fad*D Δ*adh*E::*fdh*+pTEZ+pCYPAB
Plasmid vectors	
pETDuet-1	Double T7 promoters, ColE1 ori, Amp^r
pCDFDuet-1	Double T7 promoters, CloDF13 ori, Sm^r
pTE	Derivative of pETDuet-1 with *Lreu_0335* of *Lactobacillus reuteri* DSM 20016
pTEZ	Derivative of pETDuet-1 with *Lreu_0335* and *fabZ* of *E.coli*
pCYP	Derivative of pCDFDuet-1 with CYP153A of *Marinobacter aquaeolei* VT8
pCYPAB	Derivative of pCDFDuet-1 with CYP153A and *cam*AB of *Pseudomonas putida*
pCYPR	Derivative of pCDFDuet-1 with CYP153A fused CYP102A1 reductase

USA) donated by Dr. Hiroshi Sakamoto (Pasteur Institute, France) were used for cloning and sub-cloning. *E. coli* strains DH5α and BW25113 were cultured in Luria-Bertani (LB, Difco) broth or on an agar plate supplemented with the appropriate amount of antibiotics. M9 minimal media were used for biotransformation from glucose to FFA and HFA production. Super optimal broth (SOB) and super optimal broth with catabolite repression (SOC) media were prepared as described elsewhere (Hanahan 1983). *L. reuteri* DSM 20016, *M. aquaeolei* VT8 (ATCC 700491), *P. putida* ATCC 17453, and *C. boidinii* ATCC 56294 were purchased from Deutsche Sammlung von Mikroorganismen und Zellkulturen GmbH (DSMZ) and the American Type Culture Collection (ATCC).

All extraction solvents, FFA (C_{16}, C_{18}), and ω-HPA were purchased from Sigma–Aldrich.

Gene deletion and manipulation method

Chromosomal DNAs from *L. reuteri* DSM 20016, *M. aquaeolei* VT8, *P. putida* ATCC 17453, and *C. boidinii* ATCC 56294 were prepared using G-spinTM for Bacteria Genomic DNA Extraction kit (iNtRON, Seungnam, South Korea). Plasmids from *E. coli* strains were prepared using the GeneAll DNA Purification System (Geneall Biotechnology, Seoul, South Korea). All polymerase chain reaction (PCR) amplifications were performed using *Pfu* polymerase with a GC II buffer (Takara Bio, Shiga, Japan). Primers used in this study were commercially synthesized by Cosmo Bioscience (Cosmo, Seoul, South Korea).

To construct the plasmid for fatty acid overproduction, *Lreu_0335* gene (GenBank accession no. NP_009513) from *L. reuteri* and *fabZ* gene from *E. coli* were obtained by PCR with the primer set of LTE-F/LTE-R (*Nde*I and *Eco*RV) and FabZ-F/FabZ-R (*Bam*H1 and *Not*I), respectively. For hydroxylation of fatty acid, overexpressing plasmids (pCYPAB) were constructed by PCR with the primer set of CYP-F/CYP-R (*Nde*I and *Xho*I), CamA-F/CamA-R (*Bam*HI and *Sac*-I), and CamB-F/CamB-R (*Nde*I and *Eco*RV). All the primer oligonucleotides used for PCR amplifications are shown in Table S2.

Genetic deletion and integration were carried out using the Red recombination system, which is a one-step inactivation system developed by Kirill et al. (Datsenko and Wanner 2000). Briefly, transformants carrying a Red helper plasmid were grown in 5-ml SOB cultures with ampicillin and L-arabinose at 30 °C to an OD_{600} of 0.6 and then made electrocompetent by concentrating 100-fold and washing three times with ice-cold 10 % glycerol. PCR products were gel purified, digested with *Dpn*I, re-purified, and suspended in elution buffer (10 mM Tris, pH 8.0). Electroporation was performed by using a Cell-Porator with a voltage booster and 0.15-mm chambers according to the manufacturer's instructions

(GIBCOyBRL) by using 25 μl of cells and 10–100 ng of PCR product. The shocked cells were added to 1 ml SOC and were then incubated 1 h at 37 °C; one half of the cells were then spread onto agar to select Cm^R or Km^R transformants. If none of the cells grew within 24 h, the remainder was spread after standing overnight at room temperature. After primary selection, mutants were kept in a medium without corresponding antibiotics. They were grown non-selectively and colony purified once at 37 °C; they were then tested for ampicillin sensitivity to test for the loss of the helper plasmid. If the plasmids were not lost, a few were then colony purified again at 43 °C and similarly tested. All primer information of the deletion and integration targets is listed in the supplemental data.

Culture and extraction of FFA and HFA

E. coli strains were inoculated into 250-ml Erlenmeyer flasks containing 50 ml of the LB medium containing 1 % glucose and a suitable concentration of antibiotics, then aerobically incubated at 37 °C on a shaker running at 200 rpm until the optical density of OD 600 nm reached approximately 0.6. For the induction of the cloned genes, 0.1-mM final concentration of isopropyl-β-D-thiogalactopyranoside (IPTG) was added to the culture and the culture was incubated at 18 °C for 16 h to produce enough biomass with protein expression. For the NADH-generating mutant strains, 0.01 M of formic acid was added to the culture after the $OD_{600\ nm}$ reached 0.8~0.9; shake flasks were then incubated at 18 °C and 200 rpm for 16 h. After the sonication of the harvested cell, P450 concentration was measured by CO affinity using an extinction coefficient of 91.9/mM/cm.

Each cell culture was harvested and extracted with the same volume of chloroform as that used for the FFA and HFA analysis by Voelker et al. (Davies 1994). After centrifugation at 13,200 rpm for 1 h, the organic layer was collected and evaporated using a SpeedVac dryer. The extracted pellet was dissolved in chloroform for gas chromatography–mass spectrometry (GC-MS).

Quantification of FFA and HFA using GC-MS

For GC-MS analysis, the isolated products were converted into their trimethylsilyl (TMS) derivatives by heating at 60 °C for 30 min with *N*,*O*-bis(trimethylsilyl)trifluoroacetamide (BSTFA). GC-MS was carried out using a Finnigan MAT system (gas chromatograph model AG3000 Trace GC Ultra ITQ1100) connected to an ion trap mass detector. The TMS derivatives were analyzed using a non-polar capillary column (5 % phenyl methyl siloxane capillary 30 m×250 μm i.d., 0.25 μm film thicknesses) and a linear temperature gradient (65 °C 1 min, temperature gradient of 15 °C/min to 250 °C, hold for 10 min, then 1 °C/min gradient to 275 °C, and hold for 2 min). The molecular mass and the FFA and HFA spectra of its derivatives were identified using GC-MS. The injector port temperature was 250 °C. The scan spectrum was 50–650 m/z, and the mass spectra were obtained by electron impact ionization at 70 eV. The other conditions were the same as those for the GC analysis mentioned above. A selected ion mode was used for the detection of FFA and HFA.

Authentic palmitic acid (C_{16}) and stearic acid (C_{18}) were analyzed using GC-MS. Five replicates of serially diluted 4 FFAs in culture media were analyzed to generate calibration curves. The retention time (RT) of palmitic acid was 12.69 min and the correlation factor was r=0.9919. The RT of stearic acid was 13.93 min and the correlation factor was r= 0.9997. The linearity was confirmed by statistical analysis (p<0.05). The RT of the authentic sample of the ω-hydroxy palmitic acid (ω-HPA) was 14.98 min, and the correlation factor was r=0.9999 (Fig. 4). Using the GC-MS database, the total ion chromatograms of the FFA4 and HFA4 strains were compared to detect HFA. All extracted samples were analyzed three times and quantified using the same method.

Quantification of intracellular cofactors using LC-MS

To quantify intracellular redox cofactors such as NAD^+ and NADH, intracellular metabolites were extracted following a previously reported method (Winder et al. 2008). Briefly, for quenching, cell culture samples were mixed with the same volume of 60 % methanol pre-chilled at −48 °C, and centrifuged for 10 min at 3000*g* and −10 °C. The pellets were dissolved using 3 ml of MeOH, frozen in liquid nitrogen, and allowed to thaw on ice three times. Extracted metabolite samples were analyzed using UPLC/triple quadrupole mass spectrometry (QQQ-MS). Liquid chromatography was performed on an Accela 1250 UPLC™ system (Thermo Fisher Scientific, USA) using a Thermo Fisher Hypersil Gold C18 column (2.1×100 mm, 1.8 μm, Thermo Fisher Scientific, USA). The temperatures of the column oven and autosampler were maintained at 30 and 10 °C, respectively. The mobile phases of the column were (A) HPLC-grade water with 0.1 % formic acid and (B) acetonitrile with 0.1 % formic acid. The linear gradient profile began with 10 % (B) for 10 min, was ramped to 90 % (B) for over 15 min, and then was step changed to the initial condition of 10 % (B), which was further maintained for 5 min. The total analysis time was 20 min at a flow rate of 200 μl/min with an injection volume of 10 μl using partial-loop mode. Mass analysis and quantification of HSL were performed using a TSQ quantum Access Max QQQ mass spectrometer (Thermo Fisher Scientific, USA). Spectra were acquired at both the positive and negative modes. The scan time for SRM transition (dwell time) was 5 ms, and each discharge current value was 4 μA between the positive and negative polarity. The conditions used for the ESI source were as follows: capillary voltage, 4.0 kV; vaporizer temperature, 40 °C; source temperature, 270 °C; and

desolvation temperature, 350 °C. Nitrogen was used as the sheath gas with a pressure of 30 psi. The parent ion of NAD^+ is 664.0 m/z and its product ion is 428.2 m/z, and the parent ion of NADH is 666.0 m/z and its product ion is 513.1 m/z. The collision energy was set at 27 eV. A Thermo Fisher Xcalibur interface was used to control mass spectrometry. Five replicates of serially diluted NAD^+ and NADH samples were analyzed to generate calibration curves. The RT of NAD^+ was 7.07 min and the correlation factor is r=0.9997. The RT of NADH was 10.97 min and the correlation factor is r=0.9983. The linearity was confirmed by statistical analysis (p<0.05).

Results

Genetic engineering for the biosynthesis of long-chain FFAs

To increase the precursor pool of HFA, thioesterase (*Lreu_0335*) from *L. reuteri* DSM20016 and β-hydroxyacetyl-ACP dehydratase (*fabZ*) from *E. coli* were overexpressed in *E. coli* BW25113 strain. FFA overproducers were constructed by the combination of pTE and pTEZ vectors (Table 1 and Fig. 1b). Various gene induction conditions such as IPTG concentration from 0.1 μM to 1 mM and induction temperatures of 18 and 30 °C for soluble co-expression of all the enzymes were examined. Additionally, the prevention of fatty acid β-oxidation by deleting acyl-CoA synthase (*fad*D) showed the highest production of FFAs (Fig. 5). The *fad*D gene was deleted successfully by one-step inactivation method with chloramphenicol resistance selection (Fig. 2a). Afterwards, the chloramphenicol resistance gene was removed by homologous recombination (Datsenko and Wanner 2000).

As a result of the quantitative GC-MS analysis, FFA1 (*Δfad*D) strain, FFA3 (*Δfad*D, ::pTEZ), and FFA4 (::pTEZ, *Δfad*D, *ΔtalA*) produced 723.9 mg/l of FFA (C_{16} 365.2 mg/l and C_{18} 358.7 mg/l), 1.01 g/l (C_{16} 503.0 mg/l and C_{18} 508.4 mg/l), and 1.08 g/l of FFA (C_{16} 508.7 mg/l and C_{18} 572.6 mg/l) which are 1.3-fold, 1.8-fold, and 2.0-fold higher than those of the WT strain, respectively (Fig. 5).

Bioconversion of C_{16}-FFA by resting *E. coli* cells with different redox systems

CYP153A from *M. aquaeolei* VT8 was used to perform regioselective hydroxylation at the ω-0 position of FFA. To compare electron transfer efficiency of class I-type with class III-type redox partners for CYP153A, two plasmids were constructed. For the class I system, pCYPAB was constructed by combining CYP153A, CamA, and CamB from *P. putida*, whereas for the class III system, pCYPR was constructed by the fusion of the CYP153A and CYP102A1 reductase domain with a linker (Fig. 3a). pCYPAB and pCYPR were transformed into *E. coli* FFA1 (*Δfad*D), generating HFA1 and HFA5 strains, respectively. When each strain cultured in LB

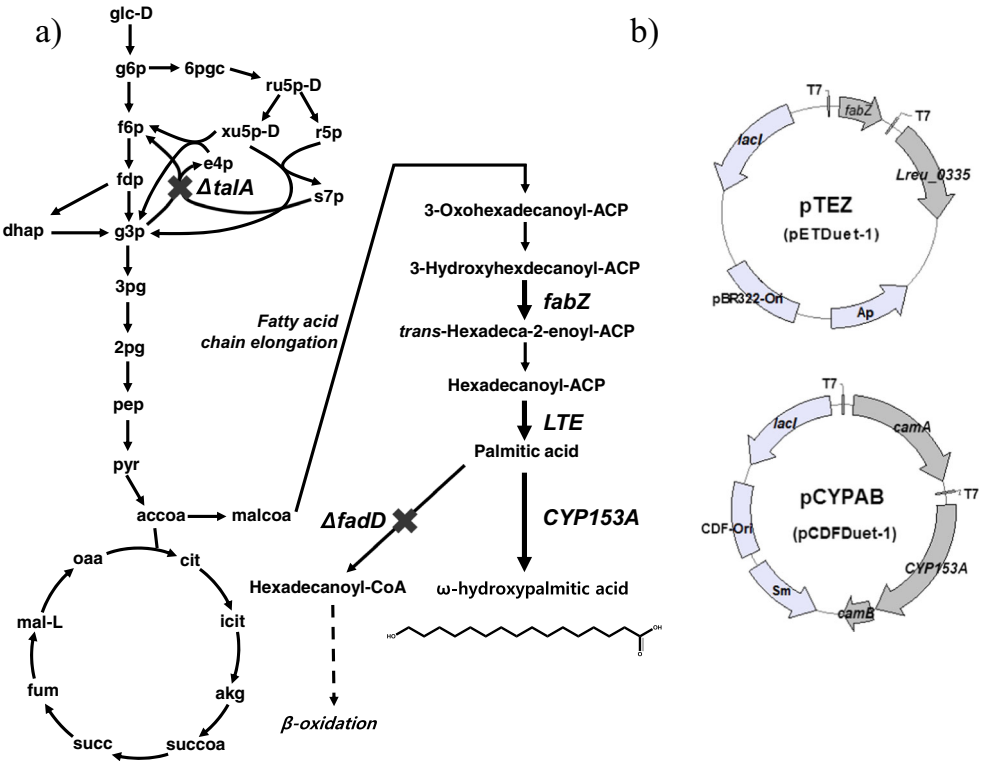

Fig. 1 **a** Schematic presentation of the strategies and **b** construction of plasmids (pTEZ containing *Lreu_0335* and *fabZ*, pCYPAB CYP153A with *cam*AB)

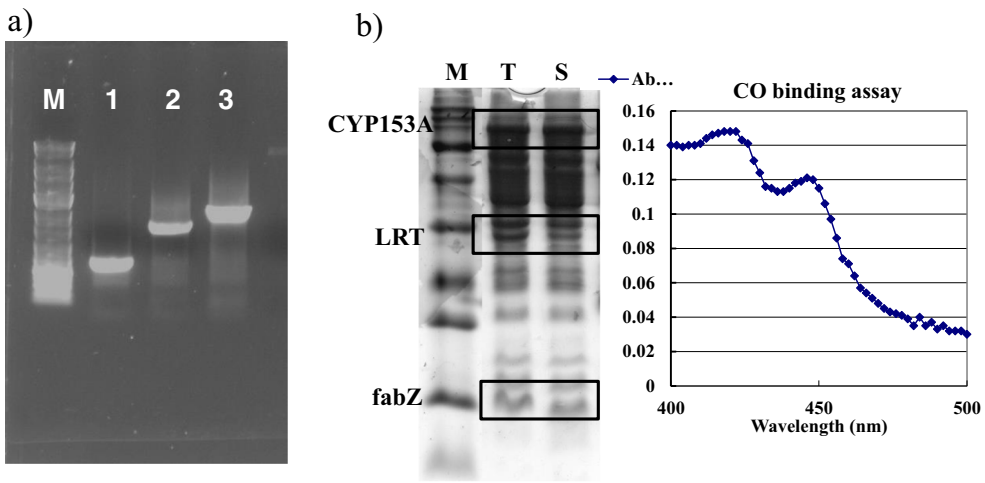

Fig. 2 **a** Gene deletion of *fad*D. *M* 1-kb ladder marker, *1* w/o chloramphenicol resistance gene with Δ*fad*D, *2* w/ chloramphenicol resistance gene with Δ*fad*D, *3 fad*D gene. **b** Detection of protein expression using SDS-PAGE (*M* broad-range marker, *T* total, *S* soluble) and CO binding of CYP153A (*X axis* wavelength, *Y axis* absorbance)

broth was induced with 0.1 mM of IPTG in the presence of 1 % glucose as elaborated in "Culture and extraction of FFA and HFA," the HFA1 strain could produce approximately 0.9 mM ω-HPA from 1 mM palmitic acid in 8 h, whereas HFA5 could produce 0.3 mM ω-HPA at the same time (Fig. 3b). HFA1 showed a 2.8-fold higher productivity than HFA5, even though the enzyme concentrations of CYP153A

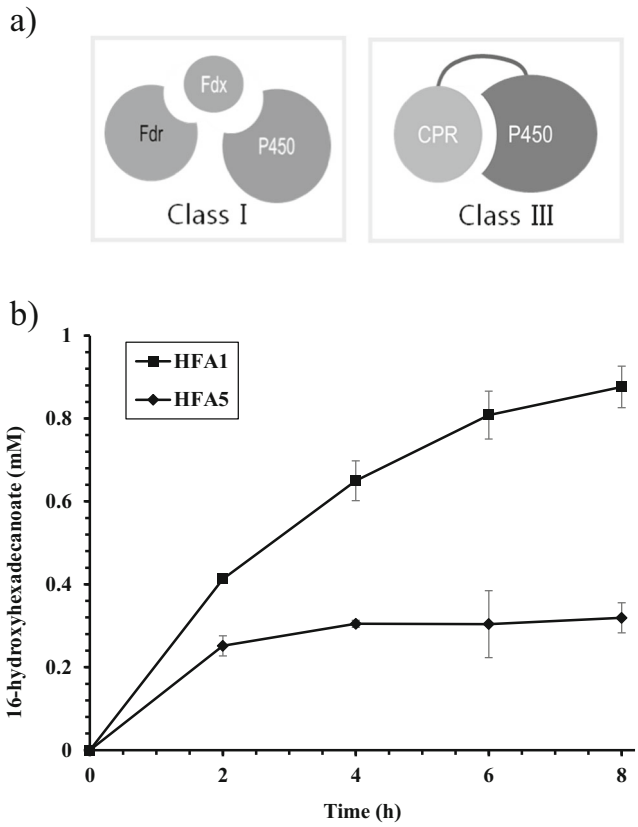

Fig. 3 **a** Redox partner construction with P450 monooxygenase (*Fdr* feredoxin reductase, *Fdx* feredoxin, *CPR* reductase domain of CYP102A1). **b** ω-Hydroxyl palmitic acid (ω-HPA) productivity between the HFA1 (Δ*fad*D+pCYPAB) and HFA5 (Δ*fad*D+pCYPR) strains

were almost the same in both *E. coli* strains according to the CO binding spectra (data not shown). One possible explanation is that the NADH concentration in the cell is much higher than the NADPH concentration, since the CamAB system mainly uses NADH as the electron donor, whereas the CYP102A1 reductase domain uses NADPH. According to the literature, NADH concentration is almost ten times higher than NADPH concentration (Andersen and von Meyenburg 1977). This result was unexpected, since the type III P450 enzyme usually shows higher activity despite a relatively low NADPH concentration owing to its high electron transfer efficiency, which suggested that linker optimization is needed for the further improvement of electron transfer efficiency.

The CamAB co-expression system was therefore used for further experiments. To combine higher ω-hydroxylation capacity and better supply of long-chain FFA as a substrate for CYP153A reaction, the FFA1~FFA4 strains mentioned in the previous section were transformed with pCYPAB vector, generating HFA1~HFA4 strains (Table 1), respectively. All of the enzymes in the HFA1~HFA4 strains were well expressed at 18 °C with 0.1 μM IPTG concentration, which was directly confirmed by SDS-PAGE and its product ω-HFA profiles (Figs. 2b and 4).

Production of ω-HPA using CYP153A

As the FFA contents increase in the HFA1~4 mutant cells, the amounts of ω-HPA in the strains were not linearly increased and reached the range of 205.0 to 212.7 mg/l. Interestingly, even though sufficient palmitic acid was supplied as a substrate for the ω-hydroxylation reaction, the HFA1~4 strains produced almost the same amount of ω-HPA, i.e., 211.7 mg/l on average (Fig. 5), suggesting that the ω-hydroxylation reaction of FFA becomes the rate-determining step (RDS). This result indicates that possible strategies to further improve the yield of ω-HPA would be any combination of the increase of the

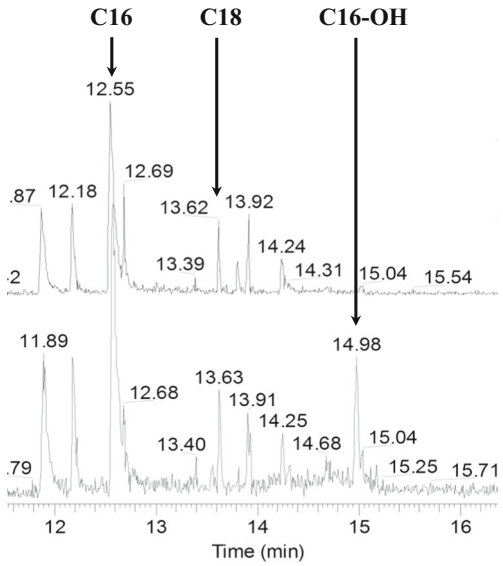

Fig. 4 Detection of ω-hydroxy palmitic acid (RT 14.98 min) using comparative analysis of TIC chromatogram from the extracted samples of the FFA4 (::pTEZ, *Δfad*D, *Δtal*A) and HFA4 (::pTEZ, ::pCYPR, *Δfad*D, *Δtal*A) strains (*up* TIC of FFA4, *down* TIC of HFA4)

expression levels of CYP153A with the CamAB system, increasing the specific activity of CYP153A, and enhancing the NADH generation system.

Although FFA (i.e., palmitic acid (C_{16}) and stearic acid (C_{18})) production in the HFA4 strain is 16 % lower than that in the FFA4 strain, the total amount of fatty acids including FFAs and ω-HPA was almost the same (Fig. 5). More precisely, when the FFA contents in the cells of the FFA4 and HFA4 strains were compared, about 104 mg/l of C_{16} and 65 mg/l of C_{18} were decreased in the HFA4 strain. On the other hand, about 210 mg/l of ω-HPA was newly produced in HFA4, while ω-hydroxy stearic acid (ω-HSA) was not detected by GC-MS. In fact, the combined amount of the decreased FFAs was about 80 % of the increased ω-HPA. These results suggest that in the HFA4 strain, more carbon sources are channeled to palmitic acid synthesis and its subsequent hydroxylation than stearic acid synthesis owing to the ω-HPA synthesis, and CYP153A appears to prefer C_{16} to C_{18} FFA as its substrate under this condition for unknown reasons.

In addition, although the deletion of *tal*A affected up to 5~6 % overproduction of FFA in the FFA4 strain, the total FFA and HPA contents in HFA4 strain are slightly lower than those in HFA3. Transaldolase belongs to the pentose phosphate pathway (PPP) that can redirect the glycolytic flux and NADPH generation. In this result, changes in the metabolism caused by the deletion of *tal*A showed insignificant effects for the HPA production in aerobic fermentation. The cause of this result is unclear. One possible explanation is that the RDS during HPA production is hydroxylated by CYP153A requiring NADH as a redox partner. Thus, HFA3 was selected for the following work to maximize NADH regeneration.

Overproduction of ω-HPA using an NADH-optimized host

For NADH overproduction in the bacteria host system, several metabolic engineering strategies were reported by blocking NADH-consuming pathways such as lactate biosynthesis and alcohol biosynthesis and integrating a NADH-generating pathway such as formate dehydrogenase (*fdh*), as

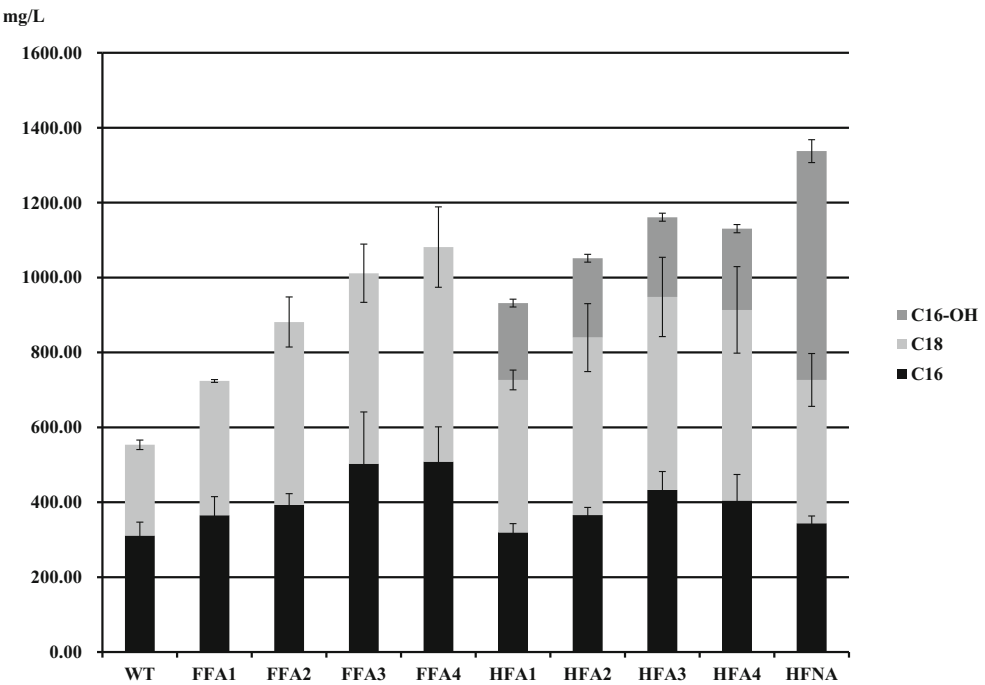

Fig. 5 Quantification of total FFAs (C_{16} and C_{18}) and ω-HPA production in genetic engineered *E. coli* strains

listed in Table 2. We constructed the NADH overproduction host using the combination of *ldh*A and *adh*E deletions, and chromosome integration of *fdh* from *C. boidinii*. Based on the result of absolute quantification of NADH and NAD^+, the ratios of NADH/NAD^+ were calculated and compared in all the mutants. To validate the redox potential profile, all mutants were sampled at two time points of fermentation after 12 h in the growth stage (Table S1) and after 16 h (Table 2), at which stage the highest producing yield of ω-HPA was shown. We expected that the DLAIF mutant (*Δldh*A, *Δadh*E, and ::*fdh*) would generate the highest amount of NADH. However, the DAIF mutant (*Δadh*E and ::*fdh*) showed the highest NADH/NAD^+ ratio, which is ca. 50 % higher than that of the wild type *E. coli* BW25113 (DE3) (Table 2). In the case of the DLAIF mutant, the mutant showed a significant growth defect, so that the DCW of DLAIF was about 50 % after 16 h, compared to the wild type *E. coli* BW25113 (DE3).

Finally, the HFNA (::*fdh*, *Δfad*D, *ΔadhE*, pTEZ, and pCYPR) strain produced 726.6 mg/l of FFAs (C_{16} 344.1 mg/l and C_{18} 382.5 mg/l) and 610.8 mg/l of ω-HPA, which is the highest production yield presented so far from glucose in *E. coli* (Fig. 5). Our results suggest that an overall twofold increase in intracellular NADH concentration in the host cell enhanced an almost 2.8-fold increase in ω-HPA. This confirms that the CYP153A reaction is the RDS in the synthesis of ω-HPA and also suggests that the NADH-reducing power supply is the rate-limiting factor in the reaction system of P450, i.e., CYP153A+CamAB.

The equilibrium of the NADH and $NADP^+$, and the NAD^+ and NADPH concentrations are tightly coupled by transhydrogenase activities, such as *pnt*AB and *udh*A. According to the literature, the intracellular cofactor ratio (i.e., NAD^+:NADH:$NADP^+$:NADPH) of *E. coli* in glucose medium with aeration fermentation is about 10:1:1:1 (Andersen and von Meyenburg 1977). Thus, dramatic changes in NADH concentration can eventually affect the concentration of NADPH via transhydrogenase. However, in this system, we expect that the NADPH concentration change in the cell through the change of NADH concentration is quite negligible, since the increase in NADH concentration only affects the hydroxylation reaction of palmitic acid.

Discussion

Previous studies were quite successful in FFA overproduction from glucose using genetic engineering strategies (Fujita et al. 2007; Ranganathan et al. 2012; Lu et al. 2008). In addition, various regio-specific hydroxylations of FFA were suggested using several different enzymes from bacteria, yeast, and fungi (Kim and Oh 2013). Although ω-*X* (*X*=1, 2, 3, 6, etc.) HFAs are important commodity chemicals for the synthesis of wax, emulsifiers, biopolymers, lubricants, and cosmetics, ω-HFA is a rare and valuable compound in fine chemical synthesis such as pseudoceramide synthesis (Park et al. 2003). Throughout this study, the ω-HPA overproduction strategy was demonstrated by maximization of both a cellular FFA synthetic pathway and a P450 reaction system for ω-hydroxylation. First, the overproduction of FFA is a prerequisite for ω-HFA overproduction by amplification of the genes involved in the fatty acid biosynthetic pathway and deletion of the genes involved in the fatty acid degradation pathway, which were well documented in the previous reports (Magnuson et al. 1993; Lu et al. 2008; Ranganathan et al. 2012). Among the candidate genes revealed, in this study, we modified the process by substituting a correct TE in ACP to accommodate and prolong the acyl chain length of our target FA (C_{16}). Second, finding efficient electron transfer partners for ω-hydroxylase P450 and their soluble overexpression would maximize the production of ω-HPA. For this purpose, CYP153A, putida redoxins, and CamAB were selected. Unexpectedly, CYP153A fusion protein with the ferredoxin reductase domain of $P450_{BM3}$(CYP102A1), which becomes an artificial self-sufficient P450 requiring NADPH cofactor, showed a lower ω-hydroxylation activity than CYP153A with co-expression of Cam*AB* requiring an NADH

Table 2 Quantification of NADH and NAD^+ in the mutants varying NADH consumption and/or regeneration

Strains	Conc. of NAD^+ (μmol/mg DCW)±SD	Conc. of NADH (μmol/mg DCW)±SD	Ratios of NADH/NAD^+	DCW[a] (mg)
E. coli BW25113 (DE3)	8.9±1.9	0.9±0.5	0.10	5
DL (Δ*ldh*A)	9.1±1.8	1.1±0.5	0.12	5
DA (Δ*adh*E)	8.7±1.2	1.1±0.3	0.12	4.5
DLA (Δ*ldh*A Δ*adh*E)	8.2±1.1	1.0±0.5	0.13	4.5
IF (::*fdh*)	9.7±1.7	1.1±0.5	0.11	4
DLIF (Δ*ldh*A ::fdh)	9.5±0.8	1.4±0.6	0.15	4
DAIL (Δ*adh*E ::fdh)	11.1±1.6	1.8±0.5	0.16	4
DLAIF (Δ*ldh*A Δ*adh*E ::fdh)	11.8±2.8	1.6±0.3	0.12	2.5

[a] Dried cell mass (DCW) was measured after 16 h of culture

cofactor. Our results suggest that not only cofactor (i.e., NADH or NADPH) specificity but also low electron transfer efficiency of the CYP153A-linker-ferredoxin reductase domain of $P450_{BM3}$ (CYP102A1) appears to be the major cause of the 2.8-fold decrease in its ω-hydroxylation activity compared to CYP153A and CamAB co-expression. Optimum linker design and efficient NAD(P)H pool regeneration might increase the ω-hydroxylation activity of the CYP153A-linker-ferredoxin reductase domain of $P450_{BM3}$ (CYP102A1) fusion protein. Third, the appropriate reduction potential cofactor NADH was maximized for CamAB to increase the electron transfer rate for CYP153A leading to ω-HPA overproduction.

NADH overproduction strategies such as the deletion of *adh*E and integration of *fdh* were therefore attempted in *E. coli* BW25113 (DE3) (Bunch et al. 1997; Berrios-Rivera et al. 2002; Echave et al. 2003). DAIF (Δ*adh*E ::fdh) showed the highest NADH/NAD^+ ratio of 0.16 and an overall twofold increase in NADH concentration in the host cell without growth defect (Table 2). On the other hand, the DLAIF (Δ*ldh*A Δ*adh*E ::fdh) strain, which was expected to be the highest NADH overproducer, showed growth defect under the same fermentation condition with 0.1 mM FA. For ω-HPA production, the HFNA strain was constructed by transforming pTEZ and pCYPAB vectors to DAIF (Δ*adh*E ::fdh) with *fad*D deletion.

Our model study focused only on the production of the ω-HPA from glucose in *E. coli*. The best strain HFNA for NADH generation and the ω-hydroxylation of FFA showed a twofold higher intracellular NADH concentration than its wild type *E. coli* BW25113 (DE3) and the highest ω-HPA product yield of 610.8 mg/l, which resulted in the highest ω-HPA production from glucose in shake flask cultures ever reported (Jin et al. 2013). As more FFAs are channeled to their corresponding ω-HFAs in the HFNA strain, the absolute amounts of biosynthesized FFAs are increased, indirectly suggesting that NADPH or precursor supply for FFA biosynthesis is still not a rate-limiting factor for the biosynthesis of FFAs, but NADH supply or CYP153 activity for the ω-HFAs biosynthesis. Although the combined total amount of biosynthesized fatty acids including both FFAs and ω-HPA in the HFNA strain was increased by ca. 18 % compared to those in the HFA4 strain, the major increase was from ω-HPA production. However, the FFA (i.e., palmitic acid (C_{16}) and stearic acid (C_{18})) productions in the HFNA strain were even 20 % lower than those in the HFA4 strain.

As expected, FFA biosynthesis in the host cell is not a RDS but is the ω-hydroxylation of FFA for the production of ω-HPA, suggesting that all the cell resources such as target protein expression and NADH cofactor regeneration should be directed and balanced towards producing more CYP153A and reducing power. Therefore, further improvement in CYP153A activity and electron transfer efficiency should be required to enhance the production of ω-HPA.

Acknowledgments This work was supported by the National Research Foundation of Korea (NRF) funded by the Ministry of Science, ICT and Future Planning (NRF-2013R1A2A2A01069197), and a grant of the Korean Health Technology R&D Project, Ministry of Health and Welfare, Republic of Korea (HN12C0055).

References

Andersen KB, von Meyenburg K (1977) Charges of nicotinamide adenine nucleotides and adenylate energy charge as regulatory parameters of the metabolism in *Escherichia coli*. J Biol Chem 252(12): 4151–4156

Berrios-Rivera SJ, Bennett GN, San KY (2002) Metabolic engineering of *Escherichia coli*: increase of NADH availability by overexpressing an NAD(+)-dependent formate dehydrogenase. Metab Eng 4(3): 217–229

Bhattarai S, Liou K, Oh TJ (2013) Hydroxylation of long chain fatty acids by CYP147F1, a new cytochrome P450 subfamily protein from *Streptomyces peucetius*. Arch Biochem Biophys. doi:10.1016/j.abb.2013.09.008

Brash AR (1999) Lipoxygenases: occurrence, functions, catalysis, and acquisition of substrate. J Biol Chem 274(34):23679–23682

Bunch PK, Mat-Jan F, Lee N, Clark DP (1997) The ldhA gene encoding the fermentative lactate dehydrogenase of *Escherichia coli*. Microbiology 143(Pt 1):187–195

Choi KY, Jung E, Yun H, Yang YH, Kim BG (2014) Engineering class I cytochrome P450 by gene fusion with NADPH-dependent reductase and *S. avermitilis* host development for daidzein biotransformation. Appl Microbiol Biotechnol. doi:10.1007/s00253-014-5706-7

Datsenko KA, Wanner BL (2000) One-step inactivation of chromosomal genes in *Escherichia coli* K-12 using PCR products. Proc Natl Acad Sci U S A 97(12):6640–6645. doi:10.1073/pnas.120163297

Davies TAHM (1994) Alteration of the specificity and regulation of fatty acid synthesis of *Escherichia coli* by expression of a plant medium-chain acyl-acyl carrier protein thioesterase. J Bacteriol 176(23): 7320–7327

Echave P, Tamarit J, Cabiscol E, Ros J (2003) Novel antioxidant role of alcohol dehydrogenase E from *Escherichia coli*. J Biol Chem 278(32):30193–30198. doi:10.1074/jbc.M304351200

Fujita Y, Matsuoka H, Hirooka K (2007) Regulation of fatty acid metabolism in bacteria. Mol Microbiol 66(4):829–839. doi:10.1111/j.1365-2958.2007.05947.x

Hanahan D (1983) Studies on transformation of *Escherichia coli* with plasmids. J Mol Biol 166(4):557–580

Handke P, Lynch SA, Gill RT (2011) Application and engineering of fatty acid biosynthesis in *Escherichia coli* for advanced fuels and chemicals. Metab Eng 13(1):28–37. doi:10.1016/j.ymben.2010.10.007

Jeon E (2012) Improved production of long-chain fatty acid in *Escherichia coli* by an engineering elongation cycle during fatty acid synthesis (FAS) through genetic manipulation. J Microbiol Biotechnol 22(7):990–999. doi:10.4014/jmb.1112.12057

Jerneren F, Oliw EH (2012) The fatty acid 8,11-diol synthase of *Aspergillus fumigatus* is inhibited by imidazole derivatives and unrelated to PpoB. Lipids 47(7):707–717. doi:10.1007/s11745-012-3673-2

Jin G, Zhang Y, Shen H, Yang X, Xie H, Zhao ZK (2013) Fatty acid ethyl esters production in aqueous phase by the oleaginous yeast *Rhodosporidium toruloides*. Bioresour Technol 150C:266–270. doi:10.1016/j.biortech.2013.10.023

Joo YC, Jeong KW, Yeom SJ, Kim YS, Kim Y, Oh DK (2012) Biochemical characterization and FAD-binding analysis of oleate

hydratase from *Macrococcus caseolyticus*. Biochimie 94(3):907–915. doi:10.1016/j.biochi.2011.12.011

Jung F, Schulz C, Blaschke F, Muller DN, Mrowietz C, Franke RP, Lendlein A, Schunck WH (2012) Effect of cytochrome P450-dependent epoxyeicosanoids on ristocetin-induced thrombocyte aggregation. Clin Hemorheol Microcirc 52(2–4):403–416. doi:10.3233/ch-2012-1614

Kim KR, Oh DK (2013) Production of hydroxy fatty acids by microbial fatty acid-hydroxylation enzymes. Biotechnol Adv. doi:10.1016/j.biotechadv.2013.07.004

Kubota M, Nodate M, Yasumoto-Hirose M, Uchiyama T, Kagami O, Shizuri Y, Misawa N (2005) Isolation and functional analysis of cytochrome P450 CYP153A genes from various environments. Biosci Biotechnol Biochem 69(12):2421–2430

Liu T, Vora H, Khosla C (2010) Quantitative analysis and engineering of fatty acid biosynthesis in *E. coli*. Metab Eng 12(4):378–386. doi:10.1016/j.ymben.2010.02.003

Lu X, Vora H, Khosla C (2008) Overproduction of free fatty acids in *E. coli*: implications for biodiesel production. Metab Eng 10(6):333–339. doi:10.1016/j.ymben.2008.08.006

Luo Y, Lee JK, Zhao H (2013) Challenges and opportunities in synthetic biology for chemical engineers. Chemical engineering science 103. doi:10.1016/j.ces.2012.06.013

Magnuson K, Jackowski S, Rock CO, Cronan JE (1993) Regulation of fatty-acid biosynthesis in *Escherichia coli*. Microbiol Rev 57(3):522–542

Matsunaga I, Yamada M, Kusunose E, Nishiuchi Y, Yano I, Ichihara K (1996) Direct involvement of hydrogen peroxide in bacterial alpha-hydroxylation of fatty acid. FEBS Lett 386(2–3):252–254

Naik SN, Goud VV, Rout PK, Dalai AK (2010) Production of first and second generation biofuels: a comprehensive review. Renew Sust Energ Rev 14(2):578–597. doi:10.1016/j.rser.2009.10.003

Nawabi P, Bauer S, Kyrpides N, Lykidis A (2011) Engineering *Escherichia coli* for biodiesel production utilizing a bacterial fatty acid methyltransferase. Appl Environ Microbiol 77(22):8052–8061. doi:10.1128/AEM.05046-11

Park BD, Youm JK, Jeong SK, Choi EH, Ahn SK, Lee SH (2003) The characterization of molecular organization of multilamellar emulsions containing pseudoceramide and type III synthetic ceramide. J Invest Dermatol 121(4):794–801. doi:10.1046/j.1523-1747.2003.12470.x

Peralta-Yahya PP, Zhang F, del Cardayre SB, Keasling JD (2012) Microbial engineering for the production of advanced biofuels. Nature 488(7411):320–328. doi:10.1038/nature11478

Ranganathan S, Tee TW, Chowdhury A, Zomorrodi AR, Yoon JM, Fu Y, Shanks JV, Maranas CD (2012) An integrated computational and experimental study for overproducing fatty acids in *Escherichia coli*. Metab Eng 14(6):687–704. doi:10.1016/j.ymben.2012.08.008

Schrewe M, Julsing MK, Lange K, Czarnotta E, Schmid A, Buhler B (2014) Reaction and catalyst engineering to exploit kinetically controlled whole-cell multistep biocatalysis for terminal FAME oxyfunctionalization. Biotechnol Bioeng. doi:10.1002/bit.25248

Shirazi MM, Kargari A, Tabatabaei M, Mostafaeid B, Akia M, Barkhi M, Shirazi MJ (2013) Acceleration of biodiesel-glycerol decantation through NaCl-assisted gravitational settling: a strategy to economize biodiesel production. Bioresour Technol 134:401–406. doi:10.1016/j.biortech.2013.02.026

Silke Schneider MGW, Dominique Sanglard, Bernard Witholt (1998) Production of chiral hydroxy long chain fatty acids by whole cell biocatalysis of pentadecanoic acid with an *E. coli* recombinant containing cytochrome P450BM-3 monooxygenase. tetrahedron: asymmetry 9:2833–2844

Van Bogaert IN, Groeneboer S, Saerens K, Soetaert W (2011) The role of cytochrome P450 monooxygenases in microbial fatty acid metabolism. FEBS J 278(2):206–221. doi:10.1111/j.1742-4658.2010.07949.x

Voll FA, Zanette AF, Cabral VF, Dariva C, Souza RO, Cardozo Filho L, Corazza ML (2012) Kinetic modeling of solvent-free lipase-catalyzed partial hydrolysis of palm oil. Appl Biochem Biotechnol 168(5):1121–1142. doi:10.1007/s12010-012-9846-x

Wang J, Chen L, Tian X, Gao L, Niu X, Shi M, Zhang W (2013) Global metabolomic and network analysis of *Escherichia coli* responses to exogenous biofuels. J Proteome Res 12(11):5302–5312. doi:10.1021/pr400640u

Wang X, Li L, Zheng Y, Zou H, Cao Y, Liu H, Liu W, Xian M (2012) Biosynthesis of long chain hydroxyfatty acids from glucose by engineered *Escherichia coli*. Bioresour Technol 114:561–566. doi:10.1016/j.biortech.2012.02.119

Winder CL, Dunn WB, Schuler S, Broadhurst D, Jarvis R, Stephens GM, Goodacre R (2008) Global metabolic profiling of *Escherichia coli* cultures: an evaluation of methods for quenching and extraction of intracellular metabolites. Anal Chem 80(8):2939–2948. doi:10.1021/ac7023409

Yan D, Lu Y, Chen YF, Wu Q (2011) Waste molasses alone displaces glucose-based medium for microalgal fermentation towards cost-saving biodiesel production. Bioresour Technol 102(11):6487–6493. doi:10.1016/j.biortech.2011.03.036